

Highly efficient gate-tunable photocurrent generation in vertical heterostructures of layered materials

Woo Jong Yu, Yuan Liu, Hailong Zhou, Anxiang Yin, Zheng Li, Yu Huang, and Xiangfeng Duan

1. Schematic illustration of the device fabrication process.

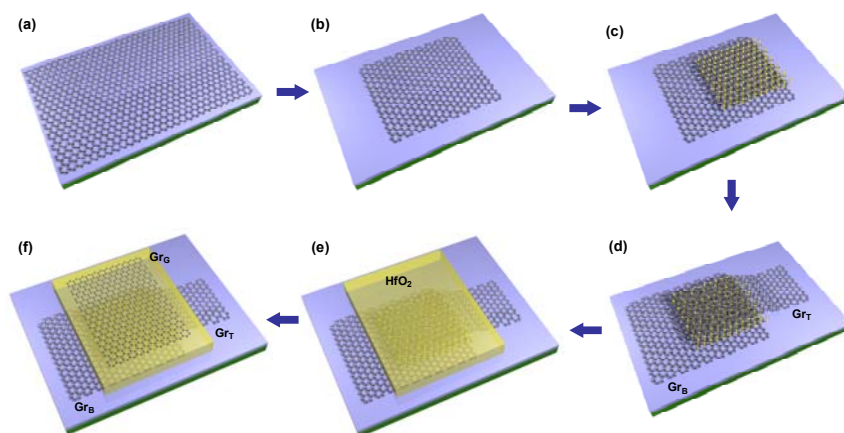


Figure S1I Schematic illustration of the device fabrication procedures. **a**, CVD grown monolayer graphene was transferred onto a 300-nm SiO₂ covered silicon substrate¹⁻⁴. **b**, Bottom graphene was patterned by oxygen plasma etching using photo resist as a etching mask. **c**, MoS₂ layer was exfoliated onto the graphene through a micromechanical cleavage approach⁵. **d**, The top graphene electrode was transferred and patterned on the MoS₂ to overlap with MoS₂ and bottom graphene. **e**, For the dual-gate heterostructures, a 60-nm of HfO₂ dielectric layer was deposited by e-beam evaporation, followed by the transferring of another graphene layer as the top-gate electrode.

2. Temporal photoresponse in the vertical graphene-MoS₂-graphene device.

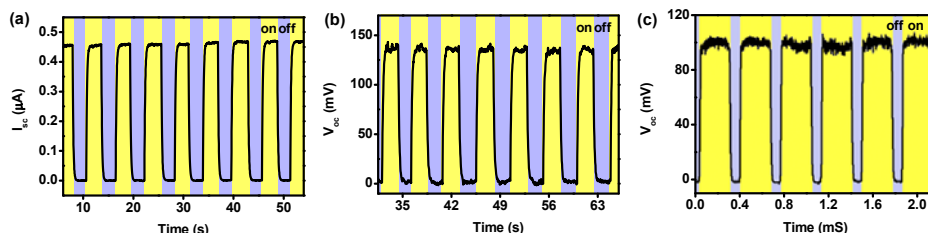


Figure S2I Temporal photoresponse in the vertical graphene-MoS₂-graphene device. **a**, Time dependent photocurrent response and **b**, Photovoltage response under a global laser (478 nm) illumination with alternatively laser on- and off-periods.. **c**, Time dependent photovoltage measurement under a global laser (478 nm) illumination through a 2.6 kHz chopper. The periodic photoresponse characteristics exhibit the same frequency as that of the laser on-off cycles. The observed photocurrent on-off transition is less than 50 μ s, which is only limited by the speed of the mechanical chopper and our measurement capability. The intrinsic speed of the photocurrent generation is likely much higher.

3. Electrical characteristics of graphene-MoS₂-graphene device.

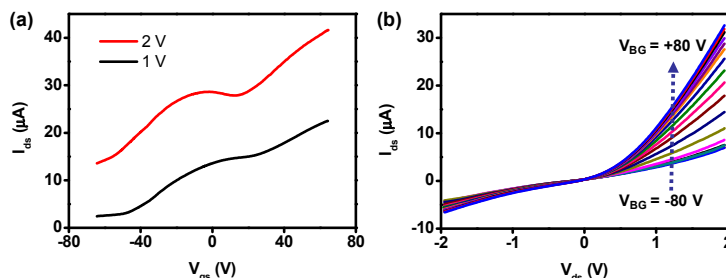


Figure S3I Electrical characteristics of graphene-MoS₂-graphene device. **a**, Transfer characteristics of graphene-MoS₂-graphene device with silicon substrate as the back-gate at $V_{ds} = 1$ V and 2 V. **b**, Output characteristics of the same device. The back-gate voltage is varied from -80 V (top) to 80 V (bottom) in the step of 10 V.

4. Simulation of the band diagram of the vertical heterostructure device.

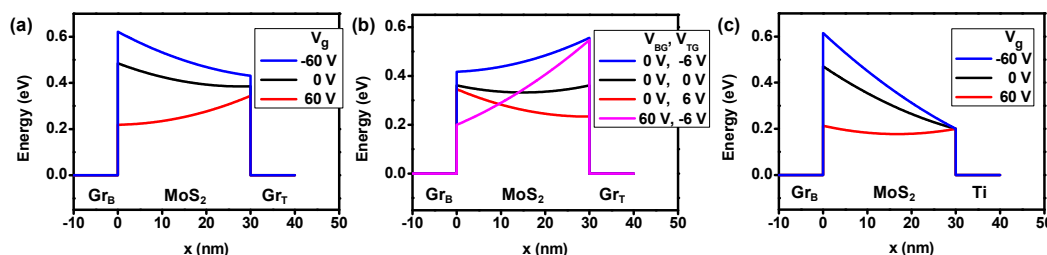


Figure S4I Simulation of the band diagrams. **a**, Simulated band diagram of single-gated graphene-MoS₂-graphene (GMG) stack. **b**, Simulated band diagram of dual-gated GMG stack. **c**, Simulated band diagram of single-gated graphene-MoS₂-Ti (GMM) stack.

To calculate the band slope and charge distribution, the configurations of GMG and GMM are considered in our simulation. Since MoS₂ is a semiconductor, we adapted the depletion approximation, which means MoS₂ is uniformly charged, and the charge density equals to its doping level. Therefore, bands of MoS₂ are parabolic instead of linear. This model is reasonable when the device channel is short, as in our cases.

For the simulation of GMG, we consider the electric field induced by gate as E_g ,

$$E_g = V_g / D \tag{1}$$

where V_g is the gate voltage and D is the thickness of SiO₂ dielectric.

Then we consider electric fields in the two graphene-MoS₂ interfaces as E_1 and E_2 . The carrier density n_1 and n_2 for bottom graphene and top graphene, respectively, can be given by:

$$\epsilon_1 E_g + \epsilon_s E_1 = n_1 e \tag{2}$$

$$\epsilon_s E_2 = n_2 e \tag{3}$$

where ϵ_1 and ϵ_s are the dielectric constant for SiO₂ and MoS₂, respectively.

E_1 and E_2 satisfy:

$$E_1 = E_2 + \frac{Ned}{\epsilon_s} \quad (4)$$

where N is the doping level in MoS₂. In our simulation, N is chosen to be 10^{17} cm^{-3} , which can be roughly estimated from transport characteristics of MoS₂ used in our study.

If we have E_1 and E_2 , we can get the potential drop ΔV in MoS₂ as:

$$\Delta V = \frac{1}{2}(E_1 + E_2)d \quad (5)$$

For graphene, we have the relation between carrier density n and chemical potential μ (Dirac point as zero) as:

$$\mu = \frac{h}{2\pi} v_F \sqrt{\pi |n - n_0|} \quad (6)$$

where h is the plank constant and v_F is the Fermi velocity, n_0 is the fixed charge graphene. As we know, intrinsic graphene in air is p-doped, and the fix charge can come from SiO₂ substrate or absorbed H₂O and O₂ molecules.

When a bias voltage V_b is applied, we get:

$$eV_b = e\Delta V + \mu_2 - \mu_1 \quad (7)$$

For GMM, it will be different because the band of MoS₂ are pinned in the metal side. Equation (7) should be replaced by:

$$eV_b = e\Delta V - \mu_1 + W_g - W_m \quad (8)$$

where W_g is the potential drop from the vacuum level to Dirac point of graphene, W_m is work function of metal. Another difference is that n_2 should be the charge density in the interface of MoS₂ and metal.

Equations above are solved self-consistently to obtain the band diagrams.

5. Simulation of gate dependant depletion width of graphene-MoS₂ schottky contact.

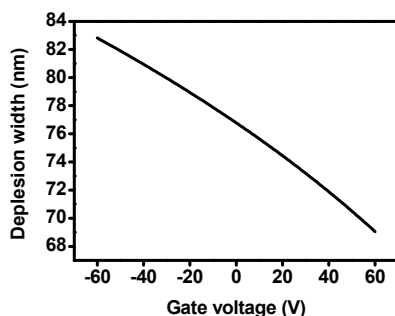


Figure S5I Simulated depletion width in graphene-MoS₂ schottky contact at the various gate voltages. In the graphene-MoS₂-graphene device, the total depletion width at both contact is doubled to be around 140-170 nm.

The electric field induced by gate E_g can be written as the following:

$$E_g = V_g / D \quad (1)$$

where V_g is the gate voltage and D is the thickness of SiO₂ dielectric.

Considering the electric field in the graphene-MoS₂ interface as E , the carrier density n for the graphene can be given by:

$$\epsilon_1 \epsilon_0 E_g + \epsilon_2 \epsilon_0 E = ne \quad (2)$$

where ϵ_1 and ϵ_2 are the dielectric constant for SiO₂ and MoS₂, respectively.

E satisfies:

$$E = \frac{Ned}{\epsilon_2 \epsilon_0} \quad (3)$$

where N is the doping level in MoS₂, and d the depletion length. In our simulation, N is chosen to be 10^{17} cm^{-3} , which can be roughly estimated from transport characteristics of MoS₂ used in our study.

We can get the potential drop ΔV in MoS₂ as:

$$\Delta V = \frac{1}{2} Ed \quad (4)$$

For graphene, we have the relation between carrier density n and chemical potential μ (Dirac point as zero) as:

$$\mu = \frac{h}{2\pi} v_F \sqrt{\pi |n - n_0|} \quad (5)$$

where h is the plank constant and v_F is the Fermi velocity, n_0 is the fixed charge graphene. As we know, intrinsic graphene in air is p-doped, and the fix charge can come from SiO₂ substrate or absorbed H₂O and O₂ molecules.

$$eV_b = e\Delta V - \mu + W_g - W_{MoS_2} \quad (6)$$

where W_g is the potential drop from the vacuum level to Dirac point of graphene, W_m is the work function (4.55 eV)⁶ of MoS₂. d is calculated by solving above equations. p-doped graphene (5.0 eV) was used in this calculation.

6. Optical absorption spectroscopy of multi-layer MoS₂ flake.

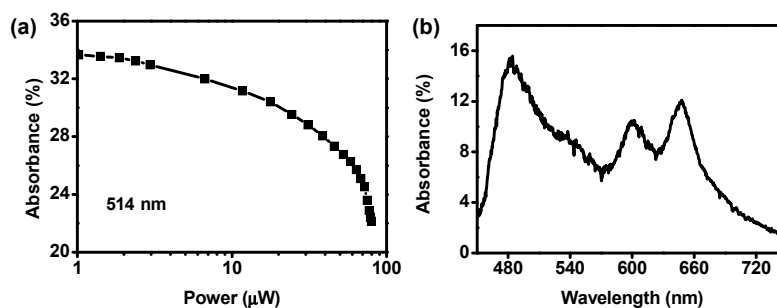


Figure S61 Optical absorption spectroscopy of multi-layer MoS₂ flake. **a**, Power dependent optical absorption of a multi-layer MoS₂ flake. The absorption was determined by comparing the focused laser (514 nm) transmission through the same glass substrate on and off an MoS₂ flake. The thickness of the MoS₂ flake is about 56 nm. **b**, Absorption spectra of a multi-layer MoS₂ flake on glass substrates. The thickness of MoS₂ flake is about 16 nm. The absorption spectra of MoS₂ was determined from the reflectance measurements^{7,8}. To obtain the absorption spectrum, the reflectance spectrum from the MoS₂ flake on a glass substrate (R_{m+s}) and that from

the same bare glass substrate (R_s) were measured using an optical microscope coupled with a spectrometer and CCD camera. The fractional change in the reflectance, δ_R , can be determined as the difference of these two quantities divided by the reflectance from the bare glass substrate ($\delta_R = \frac{R_{m+s} - R_s}{R_s}$). The absorbance of MoS₂ (A) can then be determined by using the relation: $\delta_R = \frac{4}{n_{sub}^2 - 1} A$, where n_{sub} is the refractive index of the glass substrate.

7. Schematic illustration of the fabrication procedure of graphene-MoS₂-metal (Ti) device.

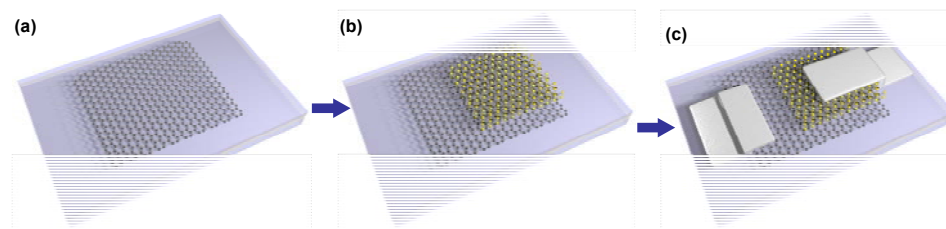


Figure S71 Schematic illustration of the fabrication procedure for graphene-MoS₂-metal (Ti) device. **a**, CVD grown monolayer graphene was transferred and patterned on the ITO glass with 30-nm Al₂O₃ dielectric layer¹⁻⁴. **b**, MoS₂ layer was exfoliated onto the graphene through a micromechanical cleavage approach⁵. **c**, As a final step, Ti/Au (50 nm/ 50 nm) was patterned as a top electrode and contact electrode for graphene using e-beam lithography.

References

1. Liu, L. *et al.* A systematic study of atmospheric pressure chemical vapor deposition growth of large-area monolayer graphene, *J. Mater. Chem.*, **22**, 1498-1503 (2012).
2. Li, X. *et al.* Large-area synthesis of high quality and uniform graphene films on copper foils. *Science* **324**, 1312-1314 (2009).
3. Reina, A. *et al.* Large area, few-layer graphene films on arbitrary substrates by chemical vapour deposition. *Nano Lett.* **9**, 30-35 (2009).
4. Zhou, H. *et al.*, Chemical vapour deposition growth of large single crystals of monolayer and bilayer graphene, *Nat. Commun.* **4**:2096, doi:10.1038/ncomms3096 (2013).
5. Radisavljevic, B., Radenovic, A., Brivio, J., Giacometti, V., Kis, A. Single-layer MoS₂ transistors. *Nature Nanotechnol.* **6**, 147-150 (2011).
6. Williams, R. H. & Mcevoy, A. J. Photoemission studies of MoS₂. *Phys. Stat. Sol. (b)* **47**, 217-224 (1971).
7. Mak, K. F., Lee, C., Hone, J., Shan, J. & Heinz & T. F. Atomically thin MoS₂: A new direct-gap semiconductor. *Phys. Rev. Lett.* **105**, 136805 (2010).
8. Mak, K. F. *et al.* Measurement of the optical conductivity of graphene. *Phys. Rev. Lett.* **101**, 196405 (2008).